

# The effective secondary electron emission coefficient of MgO protective layer in AC-PDP calculated by fitting breakdown voltage curves

Bingang Guo<sup>1,a</sup>, Chunliang Liu<sup>1</sup>, Zhongxiao Song<sup>1</sup>, Yufeng Fan<sup>1</sup>, Xing Xia<sup>1</sup>, Liu Liu<sup>1</sup>, and Duowang Fan<sup>2</sup>

<sup>1</sup> Key laboratory for Physical Electronics and Devices of the Ministry of Education of China, Xi'an Jiaotong University, P.R. China

<sup>2</sup> Key laboratory of Opto-Electronic Technology and Intelligent Control of Ministry of Education, Lanzhou Jiaotong University, P.R. China

Received: 4 November 2004 / Received in final form: 11 March 2005 / Accepted: 15 April 2005  
Published online: 18 August 2005 – © EDP Sciences

**Abstract.** A convenient way is given in this paper to calculate the effective secondary electron emission coefficient ( $\gamma_{eff}$ ) of protective layers in AC-PDP by fitting breakdown voltage curves. Based on the analysis of chemical kinetics of gas discharging in Plasma Display Panels, we deduced an empirical equation of self-sustaining discharge condition for Penning gas mixture in terms of Townsend breakdown criteria. It was used to calculate the breakdown voltage curves of Ne-Xe/MgO, Ne-Ar/MgO, Ne/MgO, Ar/MgO and Xe/MgO in a testing macroscopic discharge cell of AC-PDP. The effective secondary electron emission coefficients were derived by comparing the breakdown voltage curves obtained from the empirical equation with the experimental data of breakdown voltages. The  $\gamma_{eff}$  results showed a good conformity with the secondary electron emission coefficients in literatures. The empirical equation can be used as a convenient approach to research gas discharge characteristics and the effective secondary electron emission behaviors in plasma display panels.

**PACS.** 52.80. Sm Magnetoactive discharges (e.g., Penning discharges) – 51.50.+v Electrical properties (ionization, breakdown, electron and ion mobility, etc.)

## 1 Introduction

The secondary electron emission coefficient ( $\gamma$ ) is a very important parameter in determining the discharge characteristics in a Plasma Display Panel (PDP). The firing and sustaining voltages of PDP are largely dependent on the  $\gamma$  value of the protective layer. These voltages are closely related to the product cost and the luminous efficiency of PDP [1]. Therefore, it is very important to measure the  $\gamma$  values of protective layers in order to get better PDP performances and develop new materials with a high  $\gamma$  value. The secondary electron emission is affected by many factors when gas discharging in PDP, such as ions, excited atoms, photons, materials and surface microstructure of protective layer, and incident angle of particles. All effects influence the determination of  $\gamma$ . The combined result is always described as the effective secondary electron emission coefficient ( $\gamma_{eff}$ ) [2].

There have been many experiments and theories that attempted to determine the value of the  $\gamma_{eff}$  of protective layers in PDP. But the results are controversial because the measured or calculated values of  $\gamma_{eff}$  vary in

a rather large dispersion range [1,2]. Focused ion beam (FIB) techniques are the most common ways to characterize the secondary electron emission of the protective layer in PDPs. However, the FIB experimental conditions (ion energy, vacuum level) are very different from the PDP conditions [1–9]. The FIB results are useful only for comparative studies and not suitable for  $\gamma_{eff}$  measurements in real PDP products. Motoyama [10] reported that the total secondary emission coefficient is in between the coefficients corresponding to Auger neutralization ( $\gamma_N$ ) and Auger de-excitation ( $\gamma_D$ ) [11,12]. It gives a theoretical range of  $\gamma_{eff}$  values, but not suitable for the  $\gamma_{eff}$  measurements and corresponding studies of PDP. Another way to get  $\gamma_{eff}$  values is to estimate  $\gamma_{eff}$  by comparing the breakdown voltage curves obtained from theoretical calculation with the experimental data of breakdown voltages [2]. There are two approaches to calculate the breakdown voltage theoretically: simulation methods (e.g. Monte Carlo simulation and fluid model) and Paschen law. The convergence and the accuracy of the simulation results are closely related with the pre-setting values of parameters which are prerequisites of the computation. That always leads to great computational complexity and errors. Therefore, the

<sup>a</sup> e-mail: guobingang@ipcd.xjtu.edu.cn

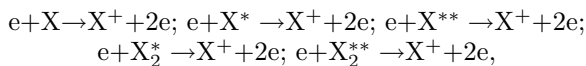
simulation methods are not suitable for convenient  $\gamma_{eff}$  measurement too. Paschen law is a convenient way to calculate breakdown voltage. It is the self-sustaining discharge condition for single gas in uniform electric field. Though most of filling gases in actual PDP products were Penning gas mixtures, many scholars still used Paschen law or other theoretical equations, which ignored the influence of Penning ionization on electron ionization coefficient  $\alpha$ , as the approximation of self-sustaining discharge condition of Penning gas mixture in their studies [13–19]. It was doubtful that whether their voltage results matched the facts. Further theoretical or modeling clarification is needed for the self-sustaining discharge condition of Penning gas mixture in  $\gamma_{eff}$  researches. Even for single filling gas, because the Paschen law does not give the clear description of the influence of metastable atoms on the secondary electron emission, and the pre-assumptions of Paschen law have some disagreements with the real discharge physics (e.g. it ignores the deionization and deexcitation processes), it may lead to some errors when calculating breakdown voltage. The Paschen law also needs theoretical modification.

On the basis of Townsend breakdown criteria and the chemical kinetics analysis of gas discharging in PDP, empirical equation of self-sustaining discharge condition for Penning gas mixture in PDP was given in this paper. The firing voltage  $V_f$  and the effective secondary electron emission coefficient  $\gamma_{eff}$  of Ne-Xe/MgO and Ne-Ar/MgO in a testing macroscopic discharge cell of AC-PDP were calculated by this empirical equation. In comparison with the voltage characteristics calculated by Paschen law and the theoretical equation which ignored the influence of Penning ionization on  $\alpha$ , the results calculated by the empirical equation had better conformity with experimental data. The empirical equation can also be used for single gas discharging. The calculated  $\gamma_{eff}$  results of Ne/MgO, Ar/MgO and Xe/MgO matched well with the results in literatures. It gave a convenient way to research gas discharge characteristics and the effective secondary electron emission behaviors in Plasma Display Panels.

## 2 Self-sustaining discharge condition of Penning gas mixture in PDP

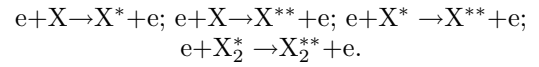
On the basis of Townsend criteria, the self-sustaining discharge condition of Penning gas mixture can be given as  $\gamma_{eff}(e^{\alpha d} - 1) = 1$ , where  $\alpha$  is directly determined by the processes of chemical kinetics of Penning gas mixture discharging in PDP. The chemical kinetics processes of Penning gas mixture discharging in PDP are shown as follows. The generation of new electrons is described by corresponding electrochemical equations.

1. Ionization impacted by an electron (direct ionization, cumulative ionization)

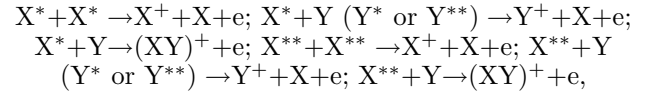


where X is a gas atom in gas mixture,  $X^*$  is an excited gas atom and  $X_2^*$  is a gas excimer. “\*\*” means cumulative excitation.

2. Excitation impacted by an electron (direct excitation, cumulative excitation)



3. Penning ionization



where Y is a gas atom whose ionization energy is less than the excitation energy of X.

4. Deionization impacted by an electron (recombination).
5. Deexcitation impacted by an electron.
6. Formation of excimers.
7. Charge transfer.
8. Excitation transfer.
9. Radiative transition.

The secondary electrons escaped from cathode surface are mainly induced by impacting ions and metastable particles, which are generated only in the first 3 processes. Consequently, coefficient  $\alpha$  should be calculated according to the first 3 processes. It includes both ionization and excitation processes. In terms of the fundamental pre-assumptions of Paschen law [20] and the additional consideration of the effects of deionization, deexcitation and electron backscattering on  $\alpha$ , the self-sustaining discharge condition of Penning gas mixture can be derived as equation (1) from the gas discharge chemical kinetics shown above.

(see equation (1) next page)

where  $P$  is filling gas pressure,  $d$  is electrodes gap distance,  $\gamma_{eff}$  is effective secondary electron emission coefficient,  $C$  and  $k_i$  ( $i = 1, 2, \dots, 16$ ) are experimental constants, which relate to gas species, gas composition and the electron energy distribution,  $U_{(X)}^i$  is ionization potential of particle X,  $U_{(X)}^*$  is excitation potential of particle X,  $U_{(X)}^{**}$  is cumulative excitation potential of particle X,  $Pr_{(X)}^i(Y)$  is ionization probability of particle X impacted by particle Y, and  $\eta_i$  ( $i = 1, 2, \dots, 10$ ) are parameters which characterize collision probability of one kind of particles impacted by an electron.  $r$  is a exponential which represents the damage effect on electron ionizing collision caused by deionization, deexcitation and electron backscattering. These damage effects on ionization become severe with increasing gas pressure  $P$  for more particle collisions [20].

There are many parameters to be determined in equation (1). It conduces to great complexity of discharge calculation directly using equation (1). It is indispensable to simplify it. After the error testing of breakdown voltages between experimental data and calculation results, the self-sustaining discharge condition of Penning gas mixture can be simplified as empirical equation (2) with satisfying calculated results. The Penning ionizations caused by metastable atoms are counted in the third item

$$\begin{aligned}
\frac{1}{CP^r d} \ln \frac{\gamma_{eff} + 1}{\gamma_{eff}} = & \exp\left(\frac{-CP^r d \cdot k_1 U_{A^i}}{U_f}\right) \cdot \eta_1 + \exp\left(\frac{-CP^r d \cdot k_2 U_{B^i}}{U_f}\right) \cdot \eta_2 + \exp\left(\frac{-CP^r d \cdot k_3 U_{(A^*)^i}}{U_f}\right) \cdot \eta_3 \\
& + \exp\left(\frac{-CP^r d \cdot k_4 U_{(B^*)^i}}{U_f}\right) \cdot \eta_4 + \exp\left(\frac{-CP^r d \cdot k_5 U_{(A^{**})^i}}{U_f}\right) \cdot \eta_5 + \exp\left(\frac{-CP^r d \cdot k_6 U_{(B^{**})^i}}{U_f}\right) \cdot \eta_6 + \exp\left(\frac{-CP^r d \cdot k_7 U_{(A_2^*)^i}}{U_f}\right) \cdot \eta_7 \\
& + \exp\left(\frac{-CP^r d \cdot k_8 U_{(B_2^*)^i}}{U_f}\right) \cdot \eta_8 + \exp\left(\frac{-CP^r d \cdot k_9 U_{(A_2^{**})^i}}{U_f}\right) \cdot \eta_9 + \exp\left(\frac{-CP^r d \cdot k_{10} U_{(B_2^{**})^i}}{U_f}\right) \cdot \eta_{10} + \exp\left(\frac{-CP^r d \cdot k_1 U_{A^*}}{U_f}\right) \cdot \eta_1 \\
& + \exp\left(\frac{-CP^r d \cdot k_2 U_{B^*}}{U_f}\right) \cdot \eta_2 + \exp\left(\frac{-CP^r d \cdot k_1 U_{A^{**}}}{U_f}\right) \cdot \eta_1 + \exp\left(\frac{-CP^r d \cdot k_2 U_{B^{**}}}{U_f}\right) \cdot \eta_2 + \exp\left(\frac{-CP^r d \cdot k_3 U_{(A^*)^{**}}}{U_f}\right) \cdot \eta_3 \\
& + \exp\left(\frac{-CP^r d \cdot k_4 U_{(B^*)^{**}}}{U_f}\right) \cdot \eta_4 + \exp\left(\frac{-CP^r d \cdot k_7 U_{(A_2^*)^{**}}}{U_f}\right) \cdot \eta_7 + \exp\left(\frac{-CP^r d \cdot k_8 U_{(B_2^*)^{**}}}{U_f}\right) \cdot \eta_8 \\
& + \exp\left(\frac{-CP^r d \cdot k_{11} U_{A^*}}{U_f}\right) \cdot Pr_{A^*}^i(A^*) \cdot \eta_1 + \exp\left(\frac{-CP^r d \cdot k_{12} U_{B^*}}{U_f}\right) \cdot Pr_{B^*}^i(B^*) \cdot \eta_2 + \exp\left(\frac{-CP^r d \cdot k_{13} U_{A^*}}{U_f}\right) \cdot Pr_{B^*}^i(A^*) \cdot \eta_1 \\
& + \exp\left(\frac{-CP^r d \cdot k_{13} U_{A^*}}{U_f}\right) \cdot Pr_{B^*}^i(A^*) \cdot \eta_1 + \exp\left(\frac{-CP^r d \cdot k_{13} U_{A^*}}{U_f}\right) \cdot Pr_{B^{**}}^i(A^*) \cdot \eta_1 + \exp\left(\frac{-CP^r d \cdot k_{14} U_{A^*}}{U_f}\right) \cdot Pr_{(AB)}^i(A^*) \cdot \eta_1 \\
& + \exp\left(\frac{-CP^r d \cdot k_{15} U_{A^{**}}}{U_f}\right) \cdot Pr_{A^{**}}^i(A^{**}) \cdot \eta_1 + \exp\left(\frac{-CP^r d \cdot k_{16} U_{B^{**}}}{U_f}\right) \cdot Pr_{B^{**}}^i(B^{**}) \cdot \eta_2 + \exp\left(\frac{-CP^r d \cdot k_{15} U_{A^{**}}}{U_f}\right) \cdot Pr_{B^*}^i(A^{**}) \cdot \eta_1 \\
& + \exp\left(\frac{-CP^r d \cdot k_{15} U_{A^{**}}}{U_f}\right) \cdot Pr_{B^*}^i(A^{**}) \cdot \eta_1 + \exp\left(\frac{-CP^r d \cdot k_{15} U_{A^{**}}}{U_f}\right) \cdot Pr_{B^{**}}^i(A^{**}) \cdot \eta_1 + \exp\left(\frac{-CP^r d \cdot k_{14} U_{A^{**}}}{U_f}\right) \cdot Pr_{(AB)}^i(A^{**}) \cdot \eta_1
\end{aligned} \tag{1}$$

of equation (2).

$$\begin{aligned}
\frac{1}{CP^r d} \ln \frac{\gamma_{eff} + 1}{\gamma_{eff}} = & \exp\left(\frac{-CP^r d \cdot K_1 U_A^i}{U_f}\right) \cdot \eta_1 \\
& + \exp\left(\frac{-CP^r d \cdot K_2 U_B^i}{U_f}\right) \cdot (1 - \eta_1) \\
& + \exp\left(\frac{-CP^r d \cdot K_3 U_A^*}{U_f}\right) \cdot \eta_1. \tag{2}
\end{aligned}$$

### 3 Experimental details

The voltage characteristics were examined in a testing macroscopic discharge cell of AC-PDP filled with gas. Figure 1a shows the schematic diagram of the testing macroscopic discharge cell of AC-PDP.  $600 \pm 50$  nm MgO films were deposited on 1 mm thick soda-lime glass substrates using e-beam evaporator. (Acceleration voltage was 6 kV, and e-beam current was 40 mA). The gas gap distance between parallel electrodes is 1 mm. AC pulse voltage was applied between electrodes X and Y. The applied rectangular voltage waveforms are shown in Figure 1b. Duty ratio is 1/1. In order to make sure that the measured breakdown voltage results were independent of frequency [21], the applied frequency can not be larger than 15 kHz in this cell structure. Here we used 12.5 kHz in breakdown voltage measurements. Sahni and Lanza [22] pointed out that the maximum sustaining voltage was the closest AC panel equivalent to the breakdown voltage. The maximum sustaining voltages were obtained by voltmeter and monitored by oscilloscope when gas igniting. In this paper, we used the measured maximum sustaining voltages as the breakdown voltage results.

The main secondary electron emission mechanism on protective layers in AC-PDP is Auger ejection in which the electron emission depends mainly on the ions potential energy and not on their kinetic energy [11, 12]. Therefore,  $\gamma_{eff}$  in equation (2) can be considered as a constant versus reduced electric field ( $E/P$ ) when identical component gas breaking down in the cell structure shown in Figure 1. Using least squares fitting method, firing voltage curve ( $V_f$  versus  $Pd$ ) measured in experiment was fitted by the self-sustaining discharge condition. As a fitting result,  $\gamma_{eff}$  could be determined when the lowest mean square fitting error was obtained.

### 4 Results and discussion

Figure 2 gives calculated firing voltage curves, which are of the lowest mean square fitting errors compared with experimental voltage results, of Penning gas mixtures: Ne+1%Xe/MgO (Fig. 2a) and Ne+1%Ar/MgO (Fig. 2b). The data points are measured values of firing voltage in experiments. The three firing voltage curves are calculated by three different self-sustaining discharge conditions:

- I: Paschen law:  $V_f = APd / \ln[BPd / \ln(1 + 1/\gamma_{eff})]$  [17],
  - II:  $\gamma_{eff} [\exp(\alpha d) - 1] = 1$ ,  $\alpha = \eta \alpha_{Ne} + (1 - \eta) \alpha_{Xe/Ar}$  ( $0 \leq \eta \leq 1$ ),  $\alpha = C' P \exp[-DP/E]$  [16, 23], and
  - III: empirical equation (2).
- $A$ ,  $B$ ,  $C'$  and  $D$  are experimental constants.

The lowest mean square error  $S^2$  ( $S^2 = \frac{1}{n-1} \sum_{i=1}^n (U_{f_i-cal} - U_{f_i-meas})^2$ ) of least squares fitting between calculated firing voltage values and measured firing voltage values and other parameters are given

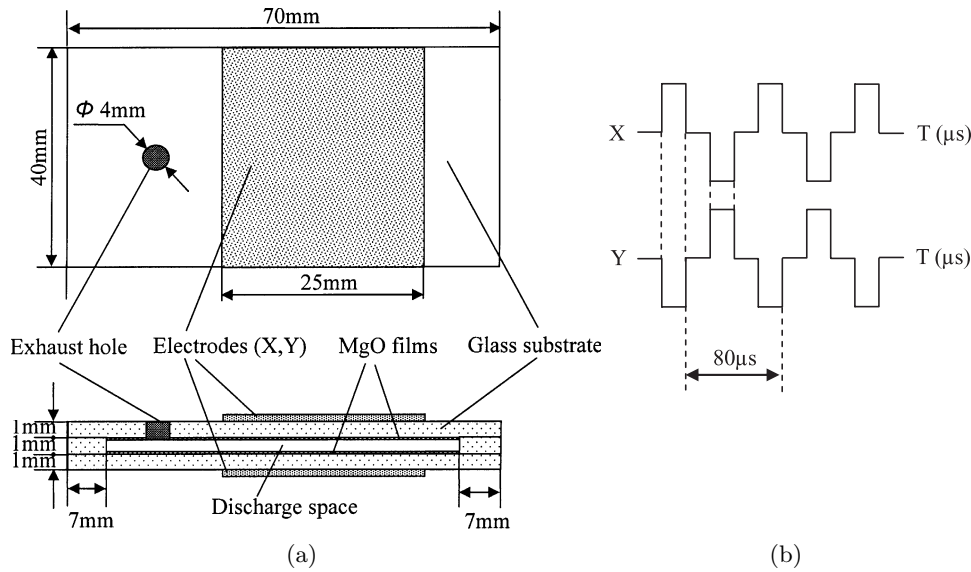


**Fig. 1.** (a) Schematic diagram of testing macroscopic discharge cell of AC-PDP. (b) The applied rectangular voltage waveforms.

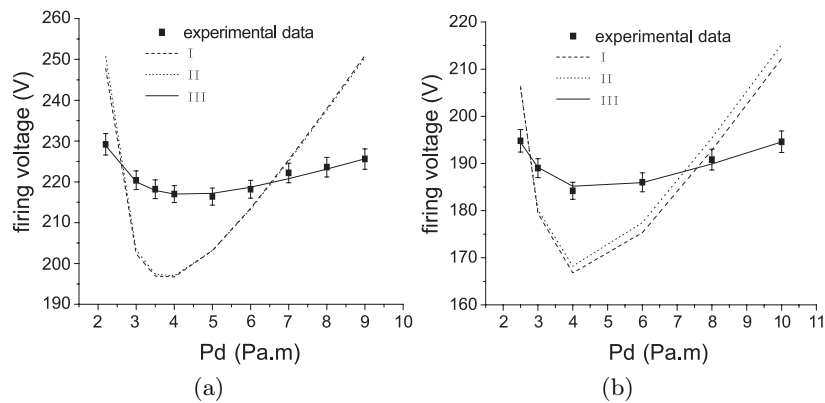


**Fig. 2.** Calculated curves of firing voltage vs.  $Pd$  for Penning gas mixture. The data points are measured values of firing voltage in experiments. (a) Ne+1%Xe/MgO, (b): Ne+1%Ar/MgO.

in Tables 1-I, 1-II and 1-III. Compared with the firing voltage curves calculated by equation I and equation II, curve III calculated by empirical equation (2) has better conformity with experimental data and much lower  $S^2$ .

Table 2 is the comparison of calculated  $\gamma_{eff}$  values of Ne-Xe/MgO with the  $\gamma$  values in literatures.  $\gamma$  values in references [17,24] were measured by FIB techniques. Because the ion energy in Townsend discharging is very low [1,2,25], we selected  $\gamma$  [17,24] values when the ion energy were less than 100 eV.  $\gamma$  values in reference [2] were estimated by comparing the breakdown voltage curves obtained from fluid simulations with the experimental data of breakdown voltages. We can see that there is a good numerical conformity between  $\gamma_{eff}$  and  $\gamma$ , and there are same decreasing tendencies with increasing Xe% in  $\gamma_{eff}, \gamma$  [17, 24] and  $\gamma$  [2]. It indicates that the results calculated by empirical equation (2) characterize the discharging of Penning gas mixtures effectively.

Calculated  $\gamma_{eff}$  values of Ne-Ar/MgO are also given in Table 2.  $\gamma_{eff}$  of Ne-Ar/MgO increases obviously with a little Ar addition. There is a maximum value of  $\gamma_{eff}$  when Ar% is 1%. It indicates that there is an obvious Penning effect in Ne-Ar/MgO discharging. However,  $\gamma_{eff}$  of Ne-Xe/MgO decreases with increasing Xe%. It indicates that there is no clear Penning effect in Ne-Xe/MgO discharging. Calculated index  $r$  is always less than 1. It reveals that there is an apparent damage effect on electron ionizing collision caused by deionization, deexcitation and electron backscattering in Penning gas mixture discharging. We can also see that  $\eta_1 = 0.9 < 1$  of Ne+1%Xe/MgO and  $\eta_1 = 2.2 > 1$  of Ne+1%Ar/MgO in Table 1-III. It can be inferred that Penning ionization could be considered as an increasing of collision probability in empirical equation (2).

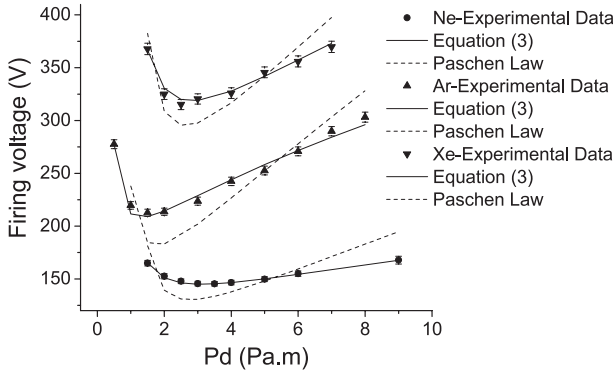
Empirical equation (1) can be simplified as the self-sustaining discharge condition for single gas, see

**Table 1.** Calculation parameters and mean square error  $S^2$  of different fitting methods.

I	$V_f = APd / \ln[BPd / \ln(1 + 1/\gamma_{eff})]$ [17]			II	$\gamma_{eff} [\exp(\alpha d) - 1] = 1, \alpha = \eta\alpha_{Ne} + (1 - \eta)\alpha_{Xe/Ar} (0 \leq \eta \leq 1), \alpha = C'P \exp[-DP/E]$ [16, 23]				
	A	B	$S^2$		$C'$	$D_{Ne}$	$D_{Xe(Ar)}$	$\eta$	$S^2$
Ne+1%Xe	52.2	2.2	323.4774	Ne+1%Xe	1.6	2.4	0.48	$\approx 1$	325.5750
Ne+1%Ar	39.6	2.4	191.3701	Ne+1%Ar	1.7	1.87	0.17	$\approx 1$	195.5285
Equation (2)									
III	C		K1	K2	K3	r	$\eta_1$	$S^2$	
Ne+1%Xe	131.9		2.4	2.4	2.5	0.432	0.9	0.4327	
Ne+1% Ar	38.7		4.58	4.52	4.54	0.466	2.2	0.3788	

**Table 2.** Comparison of calculated  $\gamma_{eff}$  values with the  $\gamma$  values in literatures.

Gas/MgO		2%	1%	0.5%	0.1%
	$\gamma$ [17, 24]	0.03–0.04	0.035–0.046	0.03–0.125	0.03–0.125
Ne+x%Xe	$\gamma$ [2]	0.12	0.22	0.48	0.66
	$\gamma_{eff}$	0.031	0.034	0.047	0.050
Ne+x%Ar	$\gamma_{eff}$	0.100	0.108	0.101	0.098

**Fig. 3.** Calculated curves of firing voltage vs.  $Pd$  for Ne/MgO, Ar/MgO and Xe/MgO by equation (3) and Paschen law. The data points are measured values of firing voltage in experiments.

equation (3). It considers both the impacting of  $A$  ions and metastable  $A$  atoms and the influence of deionization, deexcitation and electron backscattering (exponential  $r$ ).

$$\frac{1}{CP^rd} \ln \frac{\gamma_{eff} + 1}{\gamma_{eff}} = \exp\left(\frac{-CP^rd \cdot KU_A^i}{U_f}\right) + \exp\left(\frac{-CP^rd \cdot K'U_A^*}{U_f}\right). \quad (3)$$

Figure 3 gives firing voltage curves of Ne/MgO, Ar/MgO and Xe/MgO calculated by empirical equation (3) and by Paschen law [17] using least squares fitting method with the lowest mean square fitting errors  $S^2$ . The data points are measured values of firing voltage in experiments. Compared with the firing voltage curves calculated by Paschen law, the curves calculated by empirical equation (3) have better conformity with experimental data and much lower  $S^2$ . Calculated  $\gamma_{eff}$  values

and corresponding parameters of Ne/MgO, Ar/MgO and Xe/MgO are given in Table 3. Table 4 shows the secondary electron emission yield for noble gases on MgO due to Auger neutralization and Auger de-excitation processes calculated by using Hagstrum theory [10]. From the comparison of the results in Table 3 and in Table 4, we see that all the  $\gamma_{eff}$  values calculated by equation (3) are in the span of the theoretical secondary electron emission coefficients due to Auger ejection ( $\gamma_N \sim \gamma_D$ ). There are better numerical agreements between the  $\gamma_{eff}$  values calculated by equation (3) and the theoretical  $\gamma$  results in reference [10] than that between the  $\gamma_{eff}$  results calculated by Paschen law and the theoretical  $\gamma$  results in reference [10].

Therefore, the empirical equations (2, 3) can be used as a convenient approach to research gas discharge characteristics and the effective secondary electron emission behaviors in Plasma Display Panels.

## 5 Conclusions

Self-sustaining discharge condition of Penning gas mixture was given as empirical equation (2). The effective secondary electron emission coefficients can be derived by comparing the breakdown voltage curves calculated by empirical equation (2) with the experimental data of breakdown voltages. In comparison with the voltage characteristics calculated by Paschen law and the equation which ignored the influence of Penning ionization on  $\alpha$ , the voltage results calculated by empirical equation (2) had better conformity with experimental data. There was also a good conformity between  $\gamma_{eff}$  values derived from empirical equation (2) and  $\gamma$  values in literatures. It indicated that the results calculated by empirical equation (2) characterize the discharging of Penning gas mixtures

**Table 3.** Calculated  $\gamma_{eff}$  values and corresponding parameters of Ne/MgO, Ar/MgO and Xe/MgO by equation (3) and Paschen law.

Gas/MgO	equation (3)						$V_f = APd / \ln[BPd / \ln(1 + 1/\gamma_{eff})]$ [17]			
	$C$	$K$	$K'$	$r$	$\gamma_{eff}$	$S^2$	$A$	$B$	$\gamma_{eff}$	$S^2$
Ne	30.0	1.8	27.3	0.60	0.34	0.7361	47.2	1.9	0.17	239.9841
Ar	84.7	2.1	254.4	0.60	0.11	24.7829	103.1	2.9	0.18	455.9511
Xe	35.0	2.1	27.2	0.74	0.01	12.4651	112.6	2.0	0.17	348.6998

**Table 4.** Calculated values of the secondary emission coefficient ( $\gamma_N$  through Auger neutralization, and  $\gamma_D$  through resonance neutralization followed by Auger de-excitation) for MgO assuming a flat band and a Parabolic band. After Motoyama et al. [10]. In the case of rare gases on MgO,  $\gamma_i = \gamma_N$ , and  $\gamma_m = \gamma_D$  where  $\gamma_i$  and  $\gamma_m$  are the secondary electron emissions due to ion and metastable impacts respectively [10].

Gas/MgO	Ne		Ar		Xe	
$E_i, E_m$ (eV)	21.56	16.61	15.76	11.55	12.13	8.31
$\gamma$	$\gamma_N$	$\gamma_D$	$\gamma_N$	$\gamma_D$	$\gamma_N$	$\gamma_D$
Flat band	0.291	0.382	0.032	0.276	0	0.112
Parabolic band	0.279	0.382	0.012	0.273	0	0.077

effectively. Simplified empirical equation (3) was the self-sustaining discharge condition for single gas. The firing voltage curves calculated by empirical equation (3) had better conformity with experimental voltage data. The calculated  $\gamma_{eff}$  values of Ne/MgO, Ar/MgO and Xe/MgO matched well with the results calculated by Hagstrum theory in literature.

There was an apparent damage effect on electron ionizing collision caused by deionization, deexcitation and electron backscattering in gas discharging for  $r < 1$ . Penning ionization could be considered as an increasing of collision probability in empirical equation (2).

Thanks the financial support of Key Project Foundation of Ministry of Education of China (Granted No. 0205-[2002]78).

## References

- J.P. Boeuf, J. Phys. D: Appl. Phys. **36**, R53 (2003)
- Min Sup Hur, Jae Koo Lee, Hyun Chul Kim, Bong Koo Kang, IEEE T. Plasma Sci. **29**, 861, (2001)
- H. Uchiike, K. Miura, N. Nakayama, T. Shinoda, Y. Fukushima, IEEE T. Electron Dev. **ED-23**, 1211 (1976)
- N.J. Chou, J. Vac. Sci. Technol. **14**, 307 (1977)
- O. Sahni, C. Lanza, J. Appl. Phys. **47**, 1337 (1976)
- Y. Murakami, H. Matsuzaki, in *Proc. Int. Workshop on Basic Aspects of Non-equilibrium Plasmas Interacting With Surfaces (1999)*, p. 38
- E.H. Choi, H.J. Oh, Y.G. Kim, J.J. Ko, J.Y. Lim, J.G. Kim, D.I. Kim, G. Cho, S.O. Kang, Jpn J. Appl. Phys. **37**, 7015 (1998)
- D.I. Kim, J.Y. Lim, Y.G. Kim, J.J. Ko, C.W. Lee, G.S. Cho, E.H. Choi, Jpn J. Appl. Phys. **39**, 1890 (2000)
- K.S. Moon, J. Lee, K.W. Whang, J. Appl. Phys. **86**, 4049 (1999)
- Y. Motoyama, H. Matsuzaki, H. Murakami, IEEE T. Electron Dev. **ED-48**, 1568 (2001)
- H.D. Hagstrum, Phys. Rev. **104**, 672 (1956)
- H.D. Hagstrum, Phys. Rev. **122**, 83 (1961)
- C.-H. Park, W.-G. Lee, D.-H. Kim, H.-J. Ha, J.-Y. Ryu, Surf. Coat. Technol. **110**, 128 (1998)
- Z.-N. Yu, J.-W. Seo, S.-J. Yu, D.-X. Zheng, J. Sun, Surf. Coat. Technol. **162**, 11 (2002)
- H. Wenbo, S. Jian, in *Proc. ASID'00*, PB-18 (2000)
- Y. Matsunaga, T. Kato, T. Hatori, S. Hashiguchi, J. Appl. Phys. **93**, 5043 (2003)
- W.T. Lee, S.J. Im, J.G. Han, S.G. Yu, H.Y. Kim, T. Han, J.B. Yoo, K.Y. Kim, J.W. Lee, J.M. Kim, E.H. Choi, Jpn J. Appl. Phys. **41**, 6550 (2002)
- Y. Harano, K. Yoshida, H. Uchiike, IEICE Trans. Electron. **E80-C**, 1091 (1997)
- K. Yoshida, H. Uchiike, M. Sawa, IEICE Trans. Electron. **E82-C**, 1798 (1999)
- X. Xueji, Z. Dingchang, *Gas Discharging Physics* (Fudan University Press, Shanghai, 1996), p. 20, ISBN7-309-01669-6/O.165
- G.J.M. Hagelaar, M.H. Klein, R.J.M. Snijkers, G.M.W. Kroesen, J. Appl. Phys. **89**, 2033 (2001)
- O. Sahni, C. Lanza, J. Appl. Phys. **47**, 5107 (1976)
- J.P. Boeuf, C. Punset, A. Hirech, H. Doyeux, J. Phys. IV Colloq. France **7**, C4-3 (1997)
- H.S. Uhm, E.H. Choi, J.Y. Lim, Appl. Phys. Lett. **80**, 737 (2002)
- S.J. Yoon, I. Lee, J.-W. Lee, B. Oh, Jpn J. Appl. Phys. **40**, 809 (2001)